High-Latitude Topside Ionospheric Vertical Electron-Density-Profile Changes in Response to Large Magnetic Storms

Robert F. Benson[1], Joseph Fainberg[1], Vladimir A. Osherovich[2], Vladimir Truhlik[3], Yongli Wang[4], Dieter Bilitza[5], and Shing F. Fung[1]

[1]NASA/Goddard Space Flight Center, Geospace Physics Laboratory, Code 673, Heliophysics Science Division, Greenbelt, MD 20771 USA
[2]CUA/Goddard Space Flight Center, Geospace Physics Laboratory, Code 673, Heliophysics Science Division, Greenbelt, MD 20771 USA
[3]Institute of Atmospheric Physics, Academy of Sciences of the Czech Republic, Praha, Czech Republic
[4]UMBC/GPHI/Goddard Space Flight Center, Space Weather Laboratory, Code 674, Heliophysics Science Division, Greenbelt, MD 20771
[5]GMU/SWL/Goddard Space Flight Center, Heliospheric Physics Laboratory, Code 672 Heliophysics Science Division, Greenbelt, MD 20771

ABSTRACT

Large magnetic-storm induced changes have been detected in high-latitude topside vertical electron-density profiles $N_e(h)$. The investigation was based on the large database of topside $N_e(h)$ profiles and digital topside ionograms from the International Satellites for Ionospheric Studies (ISIS) program available from the NASA Space Physics Data Facility (SPDF) at http://spdf.gsfc.nasa.gov/isis/isis-status.html. This large database enabled $N_e(h)$ profiles to be obtained when an ISIS satellite passed through nearly the same region of space before, during, and after a major magnetic storm. A major goal was to relate the magnetic-storm induced high-latitude $N_e(h)$ profile changes to solar-wind parameters. Thus an additional data constraint was to consider only storms where solar-wind data were available from the NASA/SPDF OMNIWeb database. Ten large magnetic storms (with Dst less than -100 nT) were identified that satisfied both the $N_e(h)$ profile and the solar-wind data constraints. During five of these storms topside ionospheric $N_e(h)$ profiles were available in the high-latitude northern hemisphere and during the other five storms similar ionospheric data were available in the southern hemisphere. Large $N_e(h)$ changes were observed during each one of these storms. Our concentration in this paper is on the northern hemisphere. The data coverage was best for the northern-hemisphere winter. Here $N_e(h)$ profile enhancements were always observed when the magnetic local time (MLT) was between 00 and 03 and $N_e(h)$ profile depletions were always observed between 08 and 10 MLT. The observed $N_e(h)$ deviations were compared with solar-wind parameters, with appropriate time shifts, for four storms.

1. INTRODUCTION

While there have been investigations over many decades of the responses of the topside ionosphere to magnetic storms, e.g., see the review by *Warren* [1969] in the June, 1969 Proc. IEEE special issue dedicated to the International Satellites for Ionospheric Studies (ISIS) program, we seek to determine if such responses can be directly related to solar-wind (SW)

parameters. More recent works have also addressed this goal, e.g., see *Yizengaw et al*. [2006] and *Liu et al* [2010].

The motivation for this work was provided by magnetospheric electron-density (N_e) determinations during a large magnetic storm using data from the Radio Plasma Imager (RPI) on the IMAGE satellite. The RPI detected large magnetic-storm-enhanced N_e values, which were highly correlated with fluctuations in SW parameters, when IMAGE was apogee (~ $8R_E$) above the northern polar cap [*Osherovich et al.*, 2007]. Profile inversions of RPI magnetic field-aligned echoes indicated that these N_e enhancements extended down to about 4 R_E in radial distance [*Tu et al.*, 2007]. Our goal here is to extend such high-latitude investigations to even lower altitudes, i.e., into the topside ionosphere, in an attempt to relate changes in vertical electron-density profiles $N_e(h)$ to SW parameters during large magnetic storms. Ten large magnetic storms (Dst < -100 nT) were identified where high-latitude topside vertical electron-density profiles $N_e(h)$ could be obtained from Alouette/ISIS topside-sounder data and where SW data were available. Large $N_e(h)$ changes were observed during the storms in all cases. Topside-ionospheric $N_e(h)$ profiles were available in the high-latitude northern hemisphere during five of these storms and in the southern hemisphere during the other five storms. The Alouette/ISIS topside-sounder data and the SW data were obtained from the NASA Space Physics Data Facility (SPDF); the SW data from their OMNI database. Here we concentrate on the changes observed during four of the northern hemisphere storms where, in addition to good $N_e(h)$ profiles before, during, and after the storms, there was good coverage of SW data with what we considered to be the appropriate time shift.

2. HIGH-LATITUDE MAGNETIC-STORM INDUCED TOPSIDE $N_e(h)$ CHANGES

Our approach for detecting magnetic-storm-induced $N_e(h)$ changes is to obtain observations within the same small region of space before, during, and after a major magnetic storm. Such an investigation requires a large database. Here we selected restricted regions of magnetic local time (MLT), magnetic latitude (MLAT) and geographic longitude (GLON) for each storm. The restrictions on the parameter ranges were critical since too broad a range reduces the significance of the results and too small a range leads to insufficient coverage. The $N_e(h)$ profiles for the first storm investigated are based on the hand scaling of 35-mm film ionograms by skilled observers in the 1960s and 1970s during the peak activity of the ISIS program. They were obtained from the SPDF at ftp://spdf.gsfc.nasa.gov/pub/data. This was a large magnetic storm, as indicated by the Dst profile in the left panel of Figure 1, and it produced profound nighttime and daytime topside $N_e(h)$ changes as illustrated in the center and right panels, respectively.

The main features to notice in Figure 1 are the following:
(1) profiles 1 and 5 nearly coincide (before & after the storm, respectively)
(2) profile 2 (during Dst minimum) shows increase (decrease) during night (day)
(3) bifurcation of the group-2 profiles implies strong Ne gradients during Dst minimum
(4) profiles 3 and 4 are more consistently displaced during night than day.
The time separations between profiles 2a and 2b are 84 s and 39 s in the center (night) and right (day) panels, respectively, indicating rapid change in the topside ionosphere during the time of minimum Dst.

A similar presentation for the second storm investigated is presented in Figure 2.

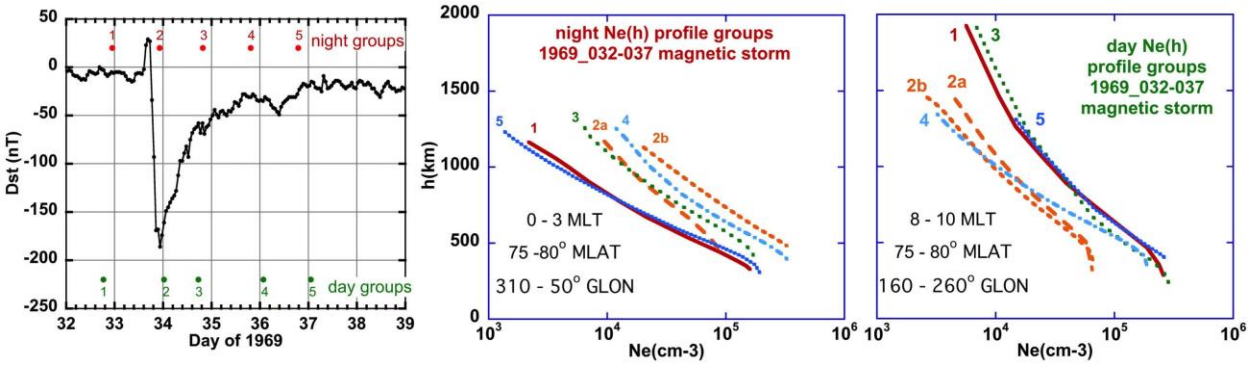

Figure 1. (left) Dst profile from the large magnetic storm during the 1969 interval from days 32 to 39 with the times for 5 groups of $N_e(h)$ profiles indicated at the top for night conditions (center panel) and at the bottom for day conditions (right panel). The profiles in the center and right panels are labeled according to the times they were collected (indicated on left panel) as they passed through the restricted region indicated in the lower left of each panel. Each profile corresponds to a single representative profile of a group of profiles collected at the time during the storm indicated in the left panel. If there were significant differences within a group two representative profiles are presented (as is the case for group 2 during the Dst minimum).

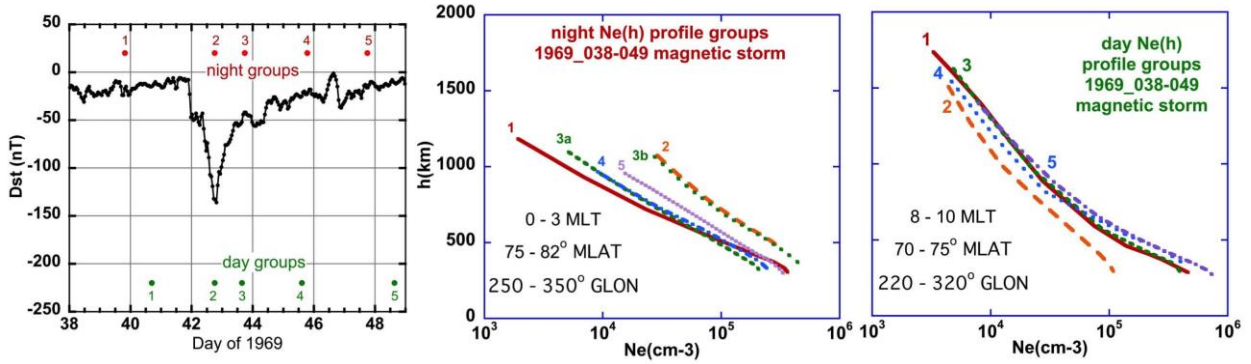

Figure 2. Same as Figure 1 except for the magnetic storm between days 38 and 49 of 1969.

In Figure 2 again, as in Figure 1, the profiles are based on earlier hand-scaling of 35-mm film ionograms and there is a large increase in the $N_e(h)$ profiles near the Dst minimum compared with pre-storm conditions (profile #2 compared with profile #1) at night (center panel) and a decrease during the day (right panel). Also, rapid changes are again indicated at night. In this case however, the greatest changes are observed early in the recovery stage where the large changes in the group-3 profiles, in the center panel of Figure 2, occur during the 30 s time separation between profiles 3a and 3b. (Profile #3b essentially coincides with profile #2.) These changes are likely due to a mixture of temporal and spatial effects since the topside sounder travels about 200 km in that time interval. The disturbed nature of this nighttime region is also indicated by the failure of the profiles, even as late as profile #5, to return to the pre-storm conditions of profile #1. In contrast, the daytime profiles (right panel) return to nearly pre-storm conditions after profile #2.

Two additional large magnetic storms, where topside ionospheric $N_e(h)$ profiles were available during northern-hemisphere spring daytime conditions, were investigated in detail. The Dst plots for these storms, and the corresponding $N_e(h)$ profiles, are presented in Figures 3 and 4. These profiles were determined from the manual scaling of digital topside ionograms from ISIS 1 and ISIS 2, respectively, obtained from http://spdf.gsfc.nasa.gov/isis/isis-status.html; they are also available from the Virtual Wave Observatory [*Fung*, 2010].

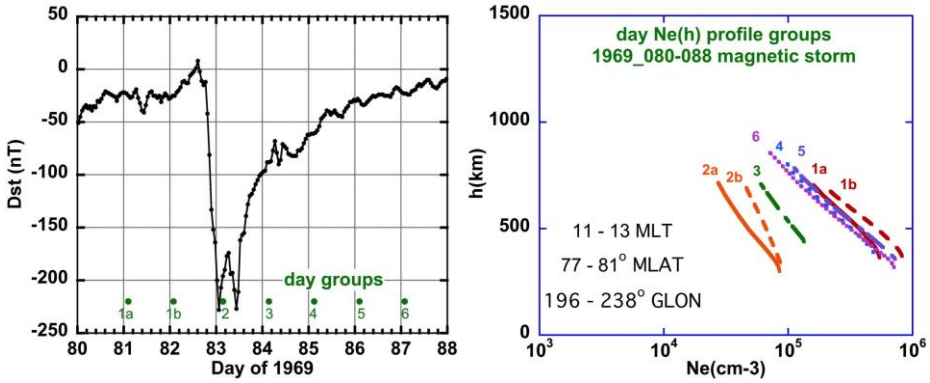

Figure 3. (left) Dst profile from the large magnetic storm during the 1969 interval from days 80 to 88 with the times for 6 groups of $N_e(h)$ profiles, obtained during day conditions, indicated at the bottom. (right) The corresponding profiles labeled according to the times they were collected (indicated on left panel) as they passed through the restricted region indicated in the lower left. Each profile corresponds to a single representative profile as described in the Figure 1 caption.

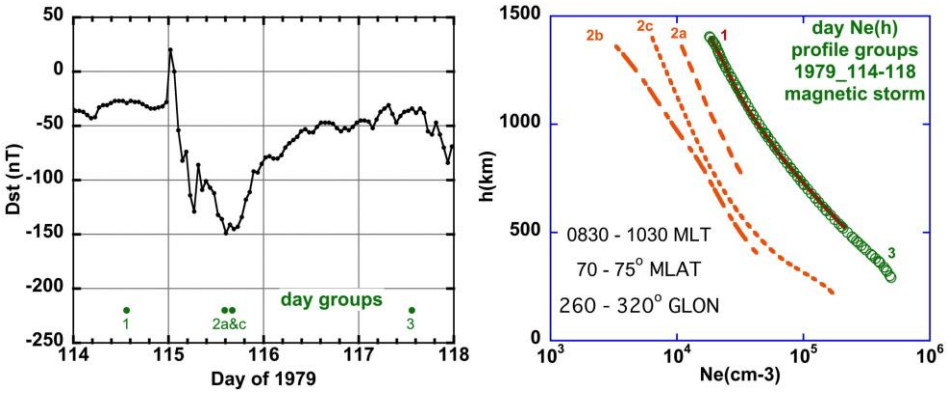

Figure 4. Same as Figure 3 except for the magnetic storm during the 1979 interval from days 114 to 118 and there are only 3 profile groups rather than 6.

The northern-hemisphere daytime $N_e(h)$ profiles for the storms indicated in Figures 3 and 4 show large decreases near the Dst minima, as were observed for the northern-hemisphere winter storms of Figures 1 and 2, and recovery to pre-storm conditions after the storm. The decreases were observed for groups 2 and 3 during the 1969 storm (Figure 3) and for groups 2a and 2c during the 1979 storm (Figure 4) and, as in Figure 1 (right panel), large changes were detected in the profiles near Dst minimum. Profiles 2a and 2b were separated by 1 min. 23 s in Figure 4 but by only 28 s in Figure 3 and the ionogram used to produce the profile 2a of Figure 3 revealed strong N_e gradients during the recording of the ionogram as illustrated in Figure 5.

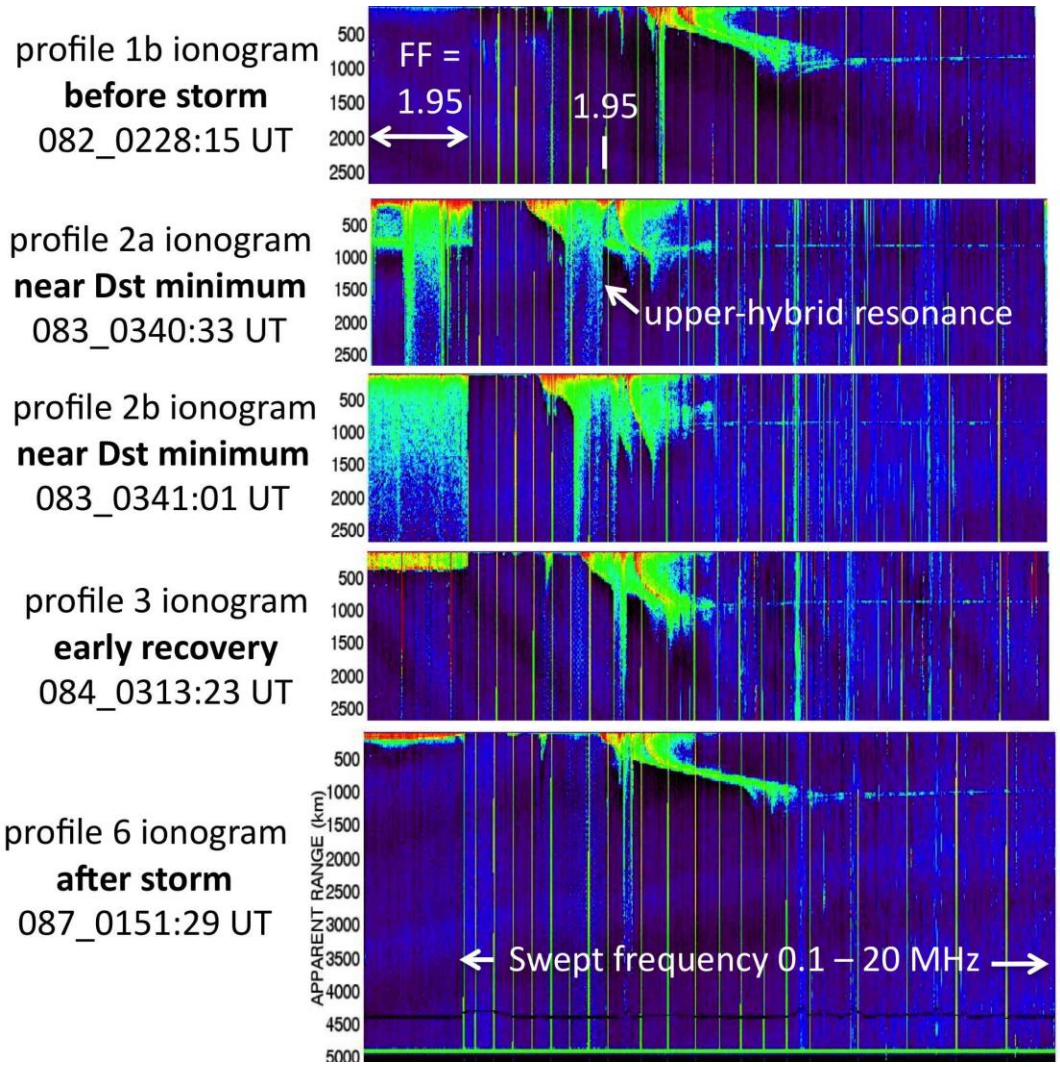

Figure 5. Portions of selected ISIS-1 ionograms used to obtain the $N_e(h)$ profiles during the magnetic storm interval from days 80 to 88 of 1969 (Figure 3) illustrating the echo shape changes during Dst minimum (compare 2a and 2b) and the rapid N_e changes within ionogram 2a as indicated by the appearance and disappearance of the upper-hybrid resonance during ~ 4 s of fixed-frequency sounding at 1.95 MHz (satellite motion ~ 30 km during this 4 s).

3. RELATING STORM-INDUCED $N_e(h)$ CHANGES TO SOLAR-WIND PARAMETERS

Figure 6 presents the SW data from OMNI 2 [*King and Papitashvili*, 2004] during the large magnetic storm of Figure 1. The behavior of the absolute value B of the total SW magnetic field **B** (top panel), the components of **B** (middle panel), and the absolute value v of the solar-wind velocity **v** (lower panel) have the characteristics of SW magnetic clouds [*Burlaga et al.*, 1981; *Osherovich and Burlaga*, 1997]. Note that in this case v, which is considered to be the most geo-effective parameter, see, e.g., *Osherovich and Fainberg* [2015], reaches a maximum near 700 km/s. In order to relate solar-wind parameters to the observed large $N_e(h)$ profile changes, presented in Section 2, it is necessary to estimate the appropriate time shift to be applied to the SW data.

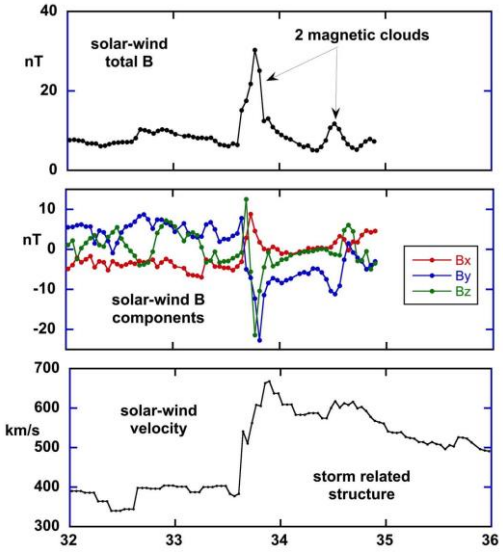

Figure 6. Solar-wind data providing evidence of magnetic clouds responsible for the magnetic storm indicated by the left panel of Figure 1.

In the work of *Osherovich et al*. [2007] there were several hours of magnetospheric N_e data near the IMAGE apogee available to compare with a similar time interval of SW data. This long time span enabled the time shift between the SW and magnetospheric N_e observations to be determined that yielded the best correlation between the two datasets. The time shift was determined to be about 3 hr. The present investigation, involving topside ionospheric satellite observations, does not contain such long data intervals from a particular restricted region. Thus a different approach was used in order to provide a reasonable estimate of the proper time shift to use between SW structures and the possibly related topside-ionospheric changes. This approach is described in a companion paper [*Osherovich and Fainberg*, 2015] where a time shift of 3.6 hr, or 0.15 days, was found. Their analysis was based on all 10 large magnetic storms identified in the present project where both the appropriate topside-sounder data and SW data were available.

The N_e change during the storms of Figures 1-4 at selected altitudes, expressed as the ratio of N_e for group 2 to group 1, are compared to the SW parameters v, B, By, and Bz (shifted by 0.15 day) in Figures 7 and 8. The ratios are very large (nearly a factor of 10 for one storm) at 1100 km for the two winter nighttime conditions (left panels) but they do not increase with increasing absolute magnitude of any of these SW parameters. The winter nighttime N_e ratios at the lower altitudes of 800 & 500 km, however, increase with increasing v, B, negative By, and negative Bz. The winter daytime N_e ratios are less than one at all altitudes (left panels) but the departures of the N_e ratios from unity increased only with increasing v and negative By. The spring daytime N_e ratios are also less than one at all altitudes (right panels) (and approach 0.1 at 550 km for one storm) and the departures of the N_e ratios from unity increased only with increasing negative Bz.

The five large magnetic storms with topside $N_e(h)$ profiles in the high-latitude southern hemisphere also revealed large storm-induced profile changes but the changes were quite different than those reported here for northern hemisphere topside ionospheric profile data and will be reported on later. Topside N_e opposite hemisphere storm-induced asymmetries have been reported earlier by *Astafyeva et al*. [2015a] and at this conference [*Astafyeva et al.*, 2015b].

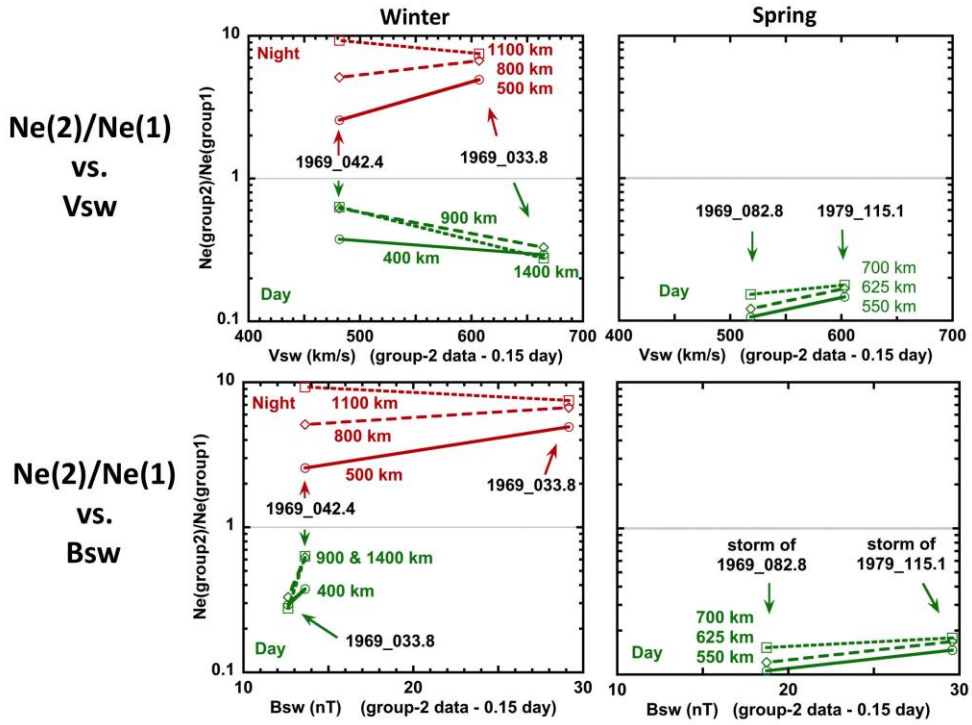

Figure 7. The ratio of N_e(group 2)/N_e(group 1) at the indicated altitudes for the magnetic storms of Figures 1 & 2 (left panels), and 3 & 4 (right panels) vs. the absolute magnitudes of the SW **v** (top) and **B** (bottom). The storm times correspond to the times when Dst first crosses -50 nT.

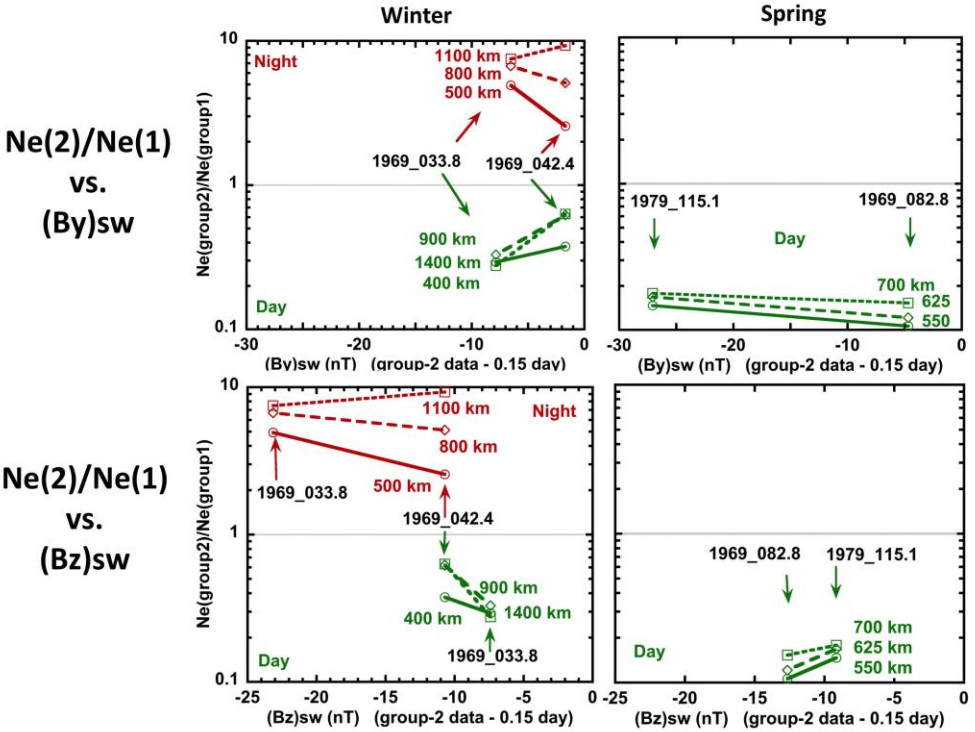

Figure 8. Same as Figure 7 except for N_e(2)/N_e(1) vs. By (top) and Bz (bottom).

4. SUMMARY

Large high-latitude ionospheric topside $N_e(h)$ changes were observed in the northern hemisphere during 4 large storms (Dst < -100 nT) investigated in detail. The magnetic-storm-induced winter $N_e(h)$ changes produced large nighttime N_e enhancements and daytime depletions in two of the storms. Daytime depletions were also observed in two spring storms. Winter nighttime enhancements at 1,100 km approached a factor of 10 and spring daytime depletions at 550 km approached a factor of 0.1. $N_e(h)$ changes within seconds were observed near the time of Dst minimum. In these storms, with good background control, the solar-wind parameters observed to influence the topside $N_e(h)$ profile changes were negative Bz in spring daytime, v and negative By in winter daytime, and v, B, negative By and negative Bz during winter night.

ACKNOWLEDGEMENTS

This work was supported by the NASA Geospace Program. V.T. was supported, in part, by grant 1507281J of the Grant Agency of the Czech Republic.

REFERENCES

Astafyeva, E., I. Zakharenkova, and E. Doornbos (2015a), Opposite hemispheric asymmetries during the ionospheric storm of 29-31 August 2004, *J. Geophys. Res. Space Physics*, *120*, doi:10.1002/2014JA020710.

Astafyeva, E., I. Zakharenkova, and E. Doornbos (2015b), Opposite hemispheric asymmetries in the ionospheric F- and topside regions observed during the geomagnetic storm of 29-31 August 2004, paper presented at Ionospheric Effects Symposium 2015, Alexandria Virginia.

Burlaga, L. F., E. Sittler, F. Mariani, and R. Schwenn (1981), Magnetic loop behind an interplanetary shock: Voyager, Helios, and IMP 8 observations, *J. Geophys. Res.*, *86*, 6673-6684.

Fung, S. F. (2010), The Virtual Wave Observatory (VWO): A portal to heliophysics wave data, *Radio Sci. Bulletin*, *No. 332*, 89-102.

King, J. H., and N. E. Papitashvili (2004), Solar wind spatial scales and comparisons of hourly Wind and ACE plasma and magnetic field data, *J. Geophys. Res.*, *110*(A2), A02209, doi:02210.01029/02004JA010804.

Liu, J., L. Liu, B. Zhao, W. Wan, and R. A. Heelis (2010), Response of the topside ionosphere to recurrent geomagnetic activity, *J. Geophys. Res.*, *115*, A12327, doi:12310.11029/12010JA015810.

Osherovich, V. A., and L. F. Burlaga (1997), Magnetic Clouds, in *Coronal Mass Ejections*, *Geophysical Monograph 99*, edited by N. Crooker, J. A. Joselyn and J. Feynman, pp. 157-168, American Geophysical Union, Washington.

Osherovich, V. A., and J. Fainberg (2015), Time delay between Dst index and magnetic storm related structure in the solar wind, *IES2015*.

Osherovich, V. A., R. F. Benson, J. Fainberg, J. L. Green, L. Garcia, S. Boardsen, N. Tsyganenko, and B. W. Reinisch (2007), Enhanced high-altitude polar-cap plasma and magnetic-field values in response to the interplanetary magnetic cloud that caused the great storm of 31 March 2001: A case study for a new magnetospheric index, *J. Geophys. Res.*, *112*, A06247, doi:06210.01029/02006JA012105.

Tu, J.-N., M. Dhar, P. Song, B. W. Reinisch, J. L. Green, R. F. Benson, and A. J. Coster (2007), Extreme polar cap density enhancements along magnetic field lines during an intense geomagnetic storm, *J.Geophys. Res*, *112*, A05201, doi:05210.01029/02006JA012034.

Warren, E. S. (1969), The topside ionosphere during geomagnetic storms, *Proc. IEEE*, *57*(6), 1029-1036.

Yizengaw, E., M. B. Moldwin, A.Komjathy, and A. J. Mannucci (2006), Unusual topside ionospheric density response to the November 2003 superstorm, *J. Geophys. Res.*, *111*, A02308, doi:02310.01029/02005JA011433.